SUMMARY OF EXPERIMENTAL UNCERTAINTY ASSESSMENT METHODOLOGY WITH EXAMPLE

by

Fred Stern, Marian Muste, Maria-Laura Beninati, and William E. Eichinger

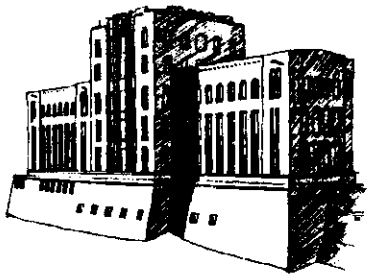

IIHR Technical Report No. 406

Iowa Institute of Hydraulic Research
College of Engineering
The University of Iowa
Iowa City, Iowa 52242

July 1999

TABLE OF CONTENTS

Abstract iii

Acknowledgments iii

1. Introduction 1

2. Test Design Philosophy 2

3. Accuracy, Errors, and Uncertainty 4

4. Measurement Systems, Data-Reduction Equations, and Error Sources 6

5. Derivation of Uncertainty Propagation Equation 8

6. Uncertainty Equations for Single and Multiple Tests 12

    6.1 Bias Limits 12

    6.2 Precision Limits for Single Tests 13

    6.3 Precision Limits for Multiple Tests 14

7. Implementation 15

8. Example for Measurement of Density and Kinematic Viscosity 16

    8.1 Test Design 17

    8.2 Measurement Systems and Procedures 18

    8.3 Test Results 20

    8.4 Uncertainty Assessment 20

        8.4.1 Multiple Tests 21

        8.4.2 Single Test 25

    8.5 Discussion of Results 27

    8.6 Comparison with Benchmark Data 28

9. Conclusions and Recommendations 32

References 34

Appendix A. Individual Variable Precision Limit 35

LIST OF FIGURES

Figure Page

1. Integration of uncertainty assessment in test process (AIAA, 1995) 3
2. Errors in the measurement of a variable X (Coleman and Steele, 1995) 5
3. Propagation of errors into experimental results (AIAA, 1995) 7
4. Sources of errors (adapted AIAA, 1995) 7
5. Schematic of error propagation from a measured variable into the result 8
6. Propagation of bias and precision errors into a two variable result (Coleman and Steele, 1995) 10
7. Experimental arrangement 17
8. Block diagram of experiment 19
9. Density of 99.7% aqueous glycerin solution test results and comparison with benchmark data 31
10. Kinematic viscosity of 99.7% aqueous glycerin solution test results and comparison with benchmark data 32

LIST OF TABLES

Table Page

1. Gravity and sphere density constants 20
2. Typical test results 20
3. Bias limits for individual variables D and t 22
4. Uncertainty estimates for density using multiple test method 23
5. Uncertainty estimates for kinematic viscosity (teflon spheres) using multiple test method 25
6. Uncertainty estimates for density using single test method 27
7. Uncertainty estimates for kinematic viscosity (teflon spheres) using single test method 27
8. Total uncertainty estimates for density and kinematic viscosity of glycerin (values in parenthesis include consideration of correlated bias errors) 28

Abstract

A summary is provided of the AIAA Standard (1995) for experimental uncertainty assessment methodology that is accessible and suitable for student and faculty use both in classroom and research laboratories. To aid in application of the methodology for academic purposes, also provided are a test design philosophy; an example for measurement of density and kinematic viscosity; and recommendations for application/integration of uncertainty assessment methodology into the test process and for documentation of results. Additionally, recommendations for laboratory administrators are included.

Acknowledgements

To insure accuracy, the summary is taken from the AIAA Standard and Coleman and Steele (1995). The work has greatly benefited from collaboration with the 22nd International Towing Tank Conference (ITTC) Resistance Committee through F. Stern. M. Muste and M. Beninati were partially supported by The University of Iowa, College of Engineering funds for fluids laboratory development and teaching assistants, respectively. Ms. A. Williams helped in data acquisition and reduction during the summer of 1998 as an undergraduate teaching assistant supported by The University of Iowa, College of Engineering funds for fluids laboratory development.

1. Introduction

Experiments are an essential and integral tool for engineering and science in general. By definition, experimentation is a procedure for testing (and determination) of a truth, principle, or effect. However, the true values of measured variables are seldom (if ever) known and experiments inherently have errors, e.g., due to instrumentation, data acquisition and reduction limitations, and facility and environmental effects. For these reasons, determination of truth requires estimates for experimental errors, which are referred to as uncertainties. Experimental uncertainty estimates are imperative for risk assessments in design both when using data directly or in calibrating and/or validating simulation methods.

Rigorous methodologies for experimental uncertainty assessment have been developed over the past 50 years. Standards and guidelines have been put forth by professional societies (ANSI/ASME, 1985) and international organizations (ISO, 1993). Recent efforts are focused on uniform application and reporting of experimental uncertainty assessment.

In particular the American Institute of Aeronautics and Astronautics (AIAA) in conjunction with Working Group 15 of the Advisory Group for Aerospace Research and Development (AGARD) Fluid Dynamics Panel has put forth a standard for assessment of wind tunnel data uncertainty (AIAA, 1995). This standard was developed with the objectives of providing a rational and practical framework for quantifying and reporting uncertainty in wind tunnel test data. The quantitative assessment method was to be compatible with existing methodologies within the technical community. Uncertainties that are difficult to quantify were to be identified and guidelines given on how to report these uncertainties. Additional considerations included: integration of uncertainty analyses into all phases of testing; simplified analysis while focusing on primary error sources; incorporation of recent technical contributions such as correlated bias errors and methods for small sample sizes; and complete professional analysis and documentation of uncertainty for each test. The uncertainty assessment methodology has application to a wide variety of engineering and scientific measurements and is based on Coleman & Steele (1995, 1999), which is an update to the earlier standards.

The purpose of this report is to provide a summary of the AIAA Standard (1995) for experimental uncertainty assessment methodology that is accessible and suitable for student and faculty use both in the classroom and in research laboratories. To aid in the application of the methodology for academic purposes, also provided are a test design philosophy; an example for measurement of density and kinematic viscosity; and recommendations for application/integration of uncertainty assessment methodology into the test process and for documentation of results. Additionally, recommendations for laboratory administrators are included.

2. Test Design Philosophy

Experiments have a wide range of purposes. Of particular interest are fluids engineering experiments conducted for science and technological advancement; research and development; design, test, and evaluation; and product liability and acceptance. Tests include small-, model-, and full-scale with facilities ranging from table-top laboratory experiments, to large-scale towing tanks and wind tunnels, to in situ experiments including environmental effects. Examples of fluids engineering tests include: theoretical model formulation; benchmark data for standardized testing and evaluation of facility biases; simulation validation; instrumentation calibration; design optimization and analysis; and product liability and acceptance.

Decisions on conducting experiments should be governed by the ability of the expected test outcome to achieve the test objectives within the allowable uncertainties. Thus, data quality assessment should be a key part of the entire experimental testing: test description, determination of error sources, estimation of uncertainty, and documentation of the results. A schematic of the experimental process, shown in Figure 1, illustrates integration of uncertainty considerations into all phases of a testing process, including the decision whether to test or not, the design of the experiments, and the conduct of the test. Along with this philosophy of testing, rigorous application/integration of uncertainty assessment methodology into the test process and documentation of results should be the foundation of all experiments.

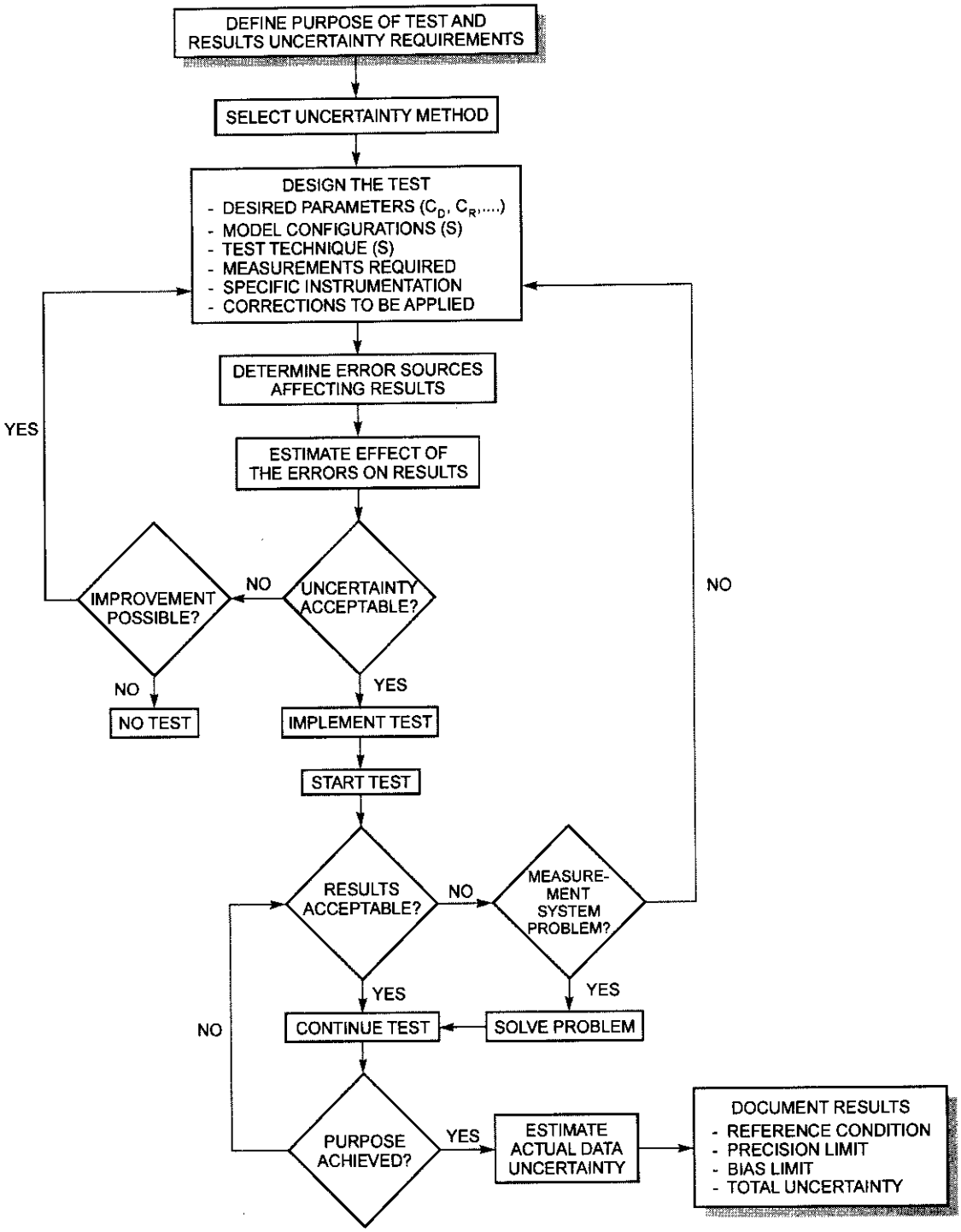

Figure 1. Integration of uncertainty assessment in test process (AIAA, 1995)

3. Accuracy, Errors, and Uncertainty

We consider here measurements made from calibrated instruments for which all known systematic errors have been removed. Even the most carefully calibrated instruments will have errors associated with the measurements, errors which we assume will be equally likely to be positive and negative. The accuracy of a measurement indicates the closeness of agreement between an experimentally determined value of a quantity and its true value. Error is the difference between the experimentally determined value and the true value. Accuracy increases as error approaches zero. In practice, the true values of measured quantities are rarely known. Thus, one must estimate error and that estimate is called an uncertainty, U. Usually, the estimate of an uncertainty, U_X, in a given measurement of a physical quantity, X, is made at a 95-percent confidence level. This means that the true value of the quantity is expected to be within the $\pm$ U interval about the mean 95 times out of 100.

As shown in Figure 2a, the total error, δ, is composed of two components: bias error, β, and precision error, ε. An error is classified as precision error if it contributes to the scatter of the data; otherwise, it is bias error. The effects of such errors on multiple readings of a variable, X, are illustrated in Figure 2b.

If we make N measurements of some variable, the bias error gives the difference between the mean (average) value of the readings, μ, and the true value of that variable. For a single instrument measuring some variable, the bias errors, β, are fixed, systematic, or constant errors (e.g., scale resolution). Being of fixed value, bias errors cannot be determined statistically. The uncertainty estimate for β is called the bias limit, B. A useful approach to estimating the magnitude of a bias error is to assume that the bias error for a given case is a single realization drawn from some statistical parent distribution of possible bias errors. The interval defined by $\pm B$ includes 95% of the possible bias errors that could be realized from the parent distribution. For example, a thermistor for which the manufacturer specifies that 95% of the samples of a given model are within $\pm$ 1.0 C° of a reference resistance-temperature calibration curve supplied with the thermistor.

The precision errors, ε, are random errors and will have different values for each measurement. When repeated measurements are made for fixed test conditions, precision errors are observed as the scatter of the data. Precision errors are due to limitations on

repeatability of the measurement system and to facility and environmental effects. Precision errors are estimated using statistical analysis, i.e., are assumed proportional to the standard deviation of a sample of N measurements of a variable, X. The uncertainty estimate of ε is called the precision limit, P.

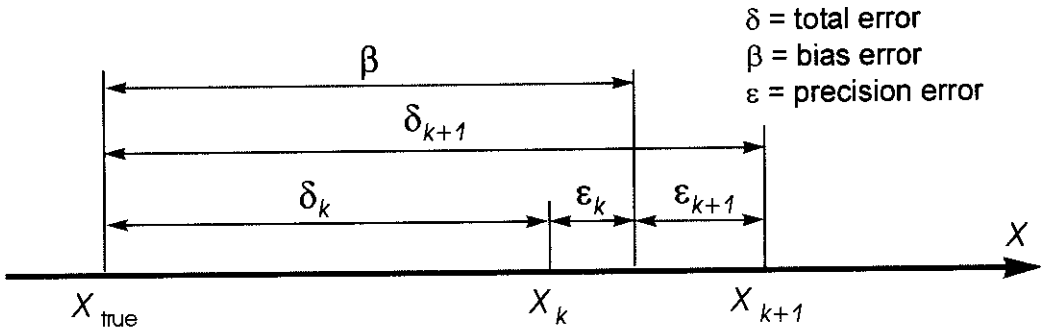

(a) two readings

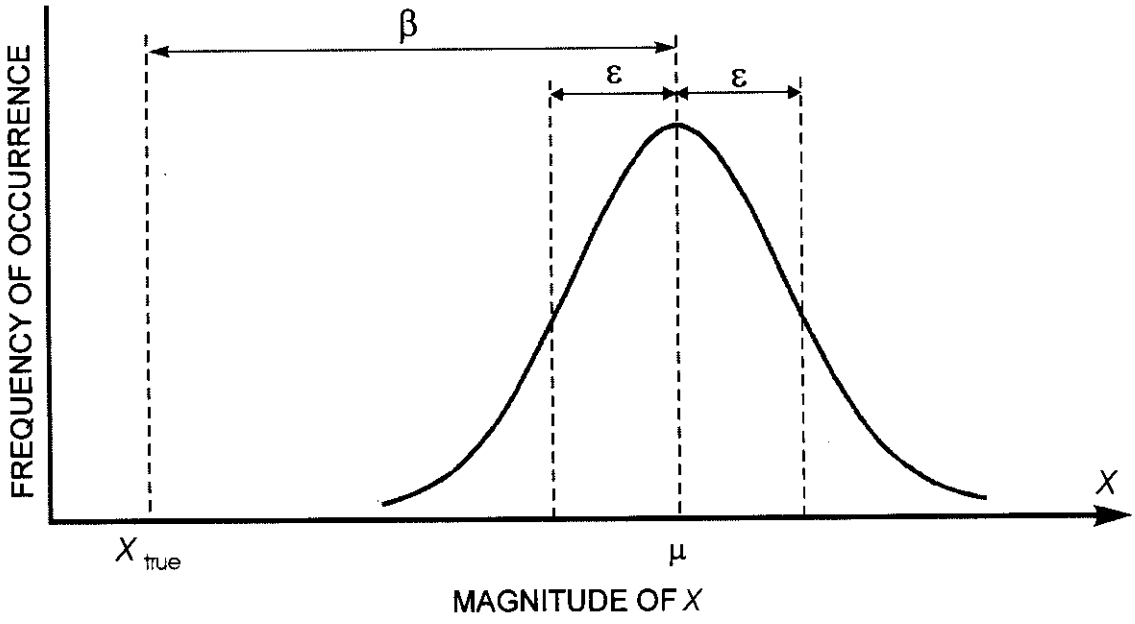

(b) infinite number of readings

Figure 2. Errors in the measurement of a variable X (Coleman and Steele, 1995)

4. Measurement Systems, Data-Reduction Equations, and Error Sources

Measurement systems consist of the instrumentation, the procedures for data acquisition and reduction, and the operational environment, e.g., laboratory, large-scale specialized facility, and in situ. Measurements are made of individual variables, X_i, to obtain a result, r, which is calculated by combining the data for various individual variables through data reduction equations

$$r = r(X_1, X_2, X_3, \ldots, X_J) \tag{1}$$

For example, to obtain the velocity of some object, one might measure the time required (X_1) for the object to travel some distance (X_2) in the data reduction equation $V = X_2 / X_1$.

Each of the measurement systems used to measure the value of an individual variable, X_i, is influenced by various elemental error sources. The effects of these elemental errors are manifested as bias errors (estimated by B_i) and precision errors (estimated by P_i) in the measured values of the variable, X_i. These errors in the measured values then propagate through the data reduction equation, thereby generating the bias, B_r, and precision, P_r, errors in the experimental result, r. Figure 3 provides a block diagram showing elemental error sources, individual measurement systems, measurement of individual variables, data reduction equations, and experimental results. Typical error sources for measurement systems are shown in Figure 4.

Estimates of errors are meaningful only when considered in the context of the process leading to the value of the quantity under consideration. In order to identify and quantify error sources, two factors must be considered: (1) the steps used in the processes to obtain the measurement of the quantity, and (2) the environment in which the steps were accomplished. Each factor influences the outcome. The methodology for estimating the uncertainties in measurements and in the experimental results calculated from them must be structured to combine statistical and engineering concepts. This must be done in a manner that can be systematically applied to each step in the data uncertainty assessment determination. In the methodology discussed below, the 95% confidence large-sample uncertainty assessment approach is used as recommended by the AIAA (1995) for the vast majority of engineering tests.

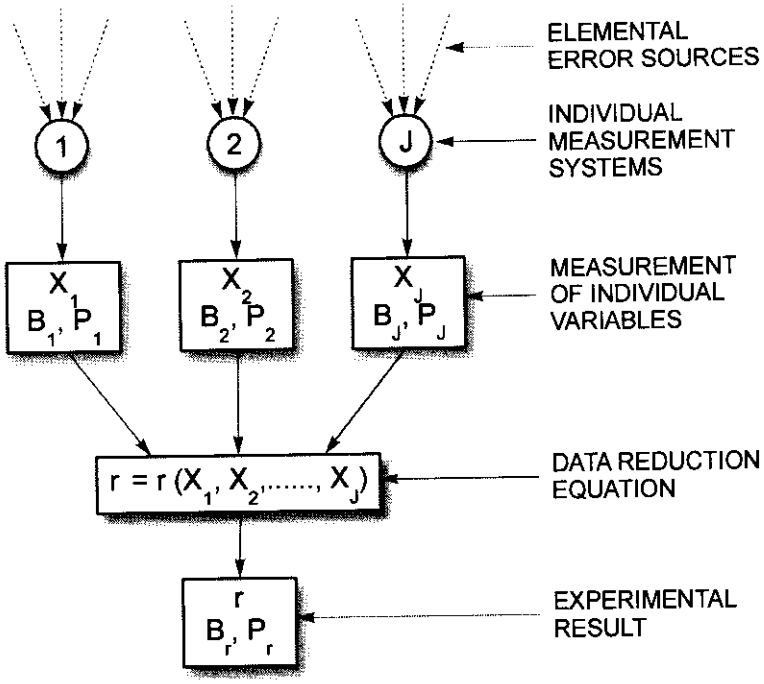

Figure 3. Propagation of errors into experimental results (AIAA, 1995)

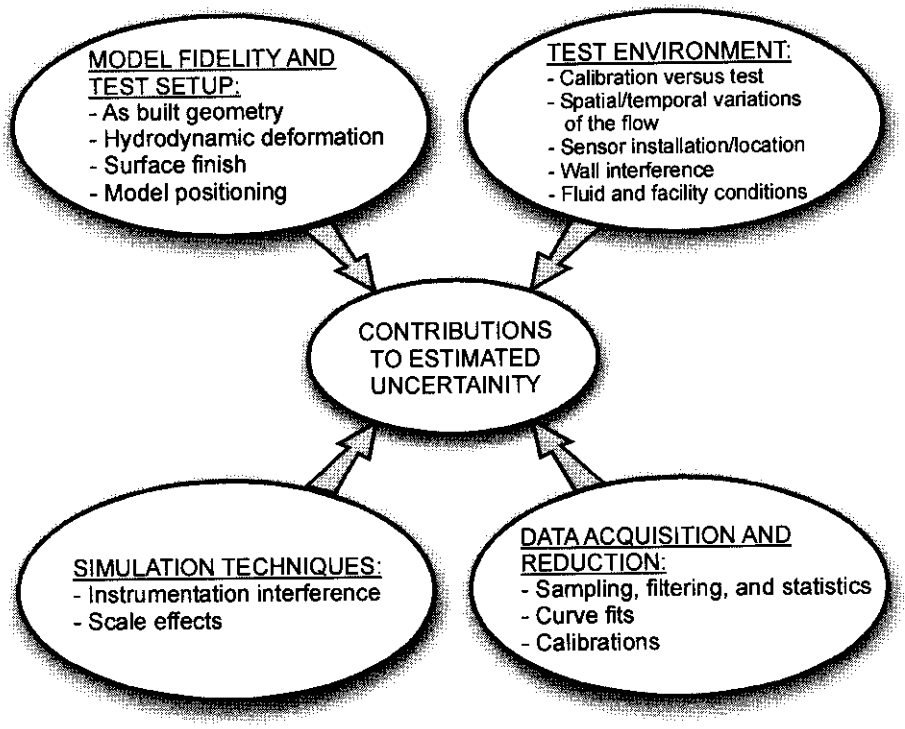

Figure 4. Sources of errors (adapted AIAA, 1995)

5. Derivation of Uncertainty Propagation Equation

Bias and precision errors in the measurement of individual variables, X_i, propagate through the data reduction equation (1) resulting in bias and precision errors in the experimental result, r (Figure 3). One can see how a small error in one of the measured variables propagates into the result by examining Figure 5. A small error, δ_{X_i}, in the measured value leads to a small error, δ_r, in the result that can be approximated using a Taylor series expansion of $r(X_i)$ about $r_{true}(X_i)$. The error in the result is given by the product of the error in the measured variable and the derivative of the result with respect to that variable dr/dX_i (i.e., slope of the data reduction equation). This derivative is referred to as a sensitivity coefficient. The larger the derivative/slope, the more sensitive the value of the result is to a small error in a measured variable.

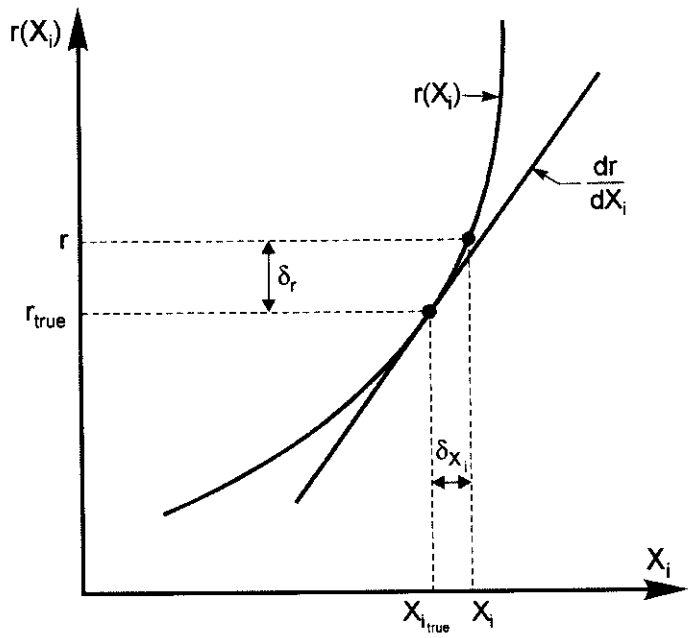

Figure 5. Schematic of error propagation from a measured variable into the result

In the following, an overview of the derivation of an equation describing the error propagation is given with particular attention to the assumptions and approximations made to obtain the final uncertainty equation applicable for both single tests and multiple

tests (Section 6). A detailed derivation can be found in Coleman and Steele (1995).

Rather than presenting the derivation for a data reduction equation of many variables, the simpler case in which equation (1) is a function of only two variables is presented, hence

$$r = r(x, y) \tag{2}$$

The situation is shown in Figure 6 for the kth set of measurements (x_k, y_k) that is used to determine r_k. Here, β_{x_k} and ε_{x_k} are the bias and precision errors, respectively, in the kth measurement of x, with a similar convention for the errors in y and r. Assume that the test instrumentation and/or apparatus is changed for each measurement so that different values of β_{x_k} and ε_{x_k} will occur for each measurement. Therefore, the bias and precision errors will be random variables relating the measured and true values

$$x_k = x_{true} + \beta_{x_k} + \varepsilon_{x_k} \tag{3}$$

$$y_k = y_{true} + \beta_{y_k} + \varepsilon_{y_k} \tag{4}$$

The error in r_k (the difference between r_{true} and r_k) in equation (2) can be approximated by a Taylor series expansion as

$$r_k - r_{true} = \frac{\partial r}{\partial x}(x_k - x_{true}) + \frac{\partial r}{\partial y}(y_k - y_{true}) + R_2 \tag{5}$$

Neglecting higher order terms (term R_2, etc.), substituting for $(x_k - x_{true})$ and $(y_k - y_{true})$ from equations (3) and (4), and defining the sensitivity coefficients $\theta_x = \partial r/\partial x$ and $\theta_y = \partial r/\partial y$, the total error δ in the kth determination of the result r is defined from equation (5) as

$$\delta_{r_k} = r_k - r_{true} = \theta_x(\beta_{x_k} + \varepsilon_{x_k}) + \theta_y(\beta_{y_k} + \varepsilon_{y_k}) \tag{6}$$

Equation (6) shows that δ_{r_k} is the product of the total errors in the measured variables (x,y) with their respective sensitivity coefficients.

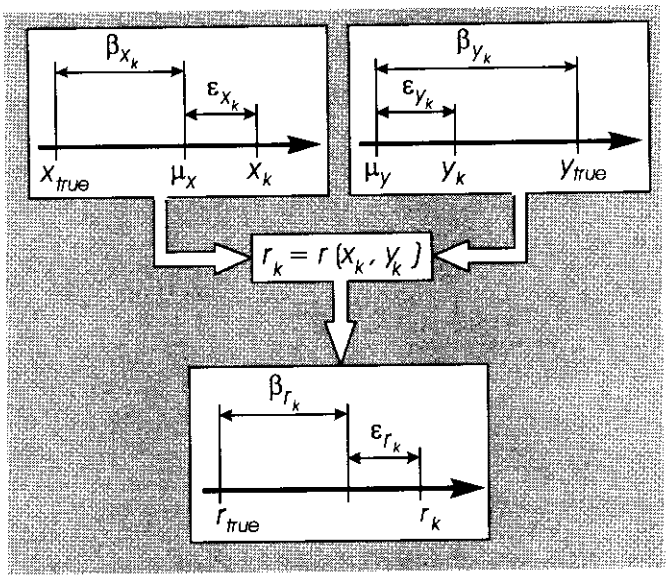

Figure 6. Propagation of bias and precision errors into a two variable result (Coleman and Steele, 1995)

We are interested in obtaining a measure of the distribution of δ_{r_k} for (some large number) N determinations of the result r. The variance of this "parent" distribution is defined by

$$\sigma_{\delta_r}^2 = \lim_{N\to\infty}\left[\frac{1}{N}\sum_{k=1}^{N}\left(\delta_{r_k}\right)^2\right]. \tag{7}$$

Substituting equation (6) into equation (7), taking the limit as N approaches infinity, using definitions of variances similar to that in equation (7) for the β's, ε's, and their correlation, and assuming that there are no bias error/precision error correlations, results in the equation for σ_{δ_r}

$$\sigma_{\delta_r}^2 = \theta_x^2\sigma_{\beta_x}^2 + \theta_y^2\sigma_{\beta_y}^2 + 2\theta_x\theta_y\sigma_{\beta_x\beta_y} + \theta_x^2\sigma_{\varepsilon_x}^2 + \theta_y^2\sigma_{\varepsilon_x}^2 + 2\theta_x\theta_y\sigma_{\varepsilon_x\varepsilon_y} \tag{8}$$

Since in reality the various σ's are not known exactly, estimates for them must be made. Defining u_c^2 as an estimate for the variance of the total error distribution, $\sigma_{\delta_r}^2$, b_x^2, b_y^2, b_{xy} as estimates for the variances and covariance of the bias error distributions,

and, S_x^2, S_y^2, S_{xy}, as estimates for the variances and covariances of the precision error distributions, results in the equation for u_c

$$u_c^2 = \theta_x^2 b_x^2 + \theta_y^2 b_y^2 + 2\theta_x \theta_y b_{xy} + \theta_x^2 S_x^2 + \theta_y^2 S_y^2 + 2\theta_x \theta_y S_{xy} \tag{9}$$

b_{xy} and S_{xy} are estimates of the correlated bias and precision errors, respectively, in x and y.

No assumptions have yet been made on types of error distributions. To obtain an uncertainty U_r at a specified confidence level (e.g., 95%), u_c must be multiplied by a coverage factor K

$$U_r = K u_c \tag{10}$$

Choosing K requires assumptions on types of error distributions. We will assume that the error distribution of the result, r, is normal so that we may replace the value of K for C% coverage (corresponding to the C% confidence level) with the t value from the Student t distribution. For sufficiently large number of measurements, $N \geq 10$, $t = 2$ for 95% confidence. With these final assumptions and generalizing equation (9) for the case in which the experimental result r is obtained from equation (1) provides the desired result

$$U_r^2 = \sum_{i=1}^{J} \theta_i^2 B_i^2 + 2\sum_{i=1}^{J-1} \sum_{k=i+1}^{J} \theta_i \theta_k B_{ik} + \sum_{i=1}^{J} \theta_i^2 P_i^2 + 2\sum_{i=1}^{J-1} \sum_{k=i+1}^{J} \theta_i \theta_k P_{ik} \tag{11}$$

where $B_i = tb_i$, $B_{ik} = t^2 b_{ik}$, $P_i = tS_i$, $P_{ik} = t^2 S_{ik}$ and $t = 2$ for $N \geq 10$. With reference to Figure 3, B_i and P_i are the bias limits in X_i; and B_{ik} and P_{ik} are the correlated bias and precision limits in X_i and X_k. S_i is the standard deviation for a sample of N readings of the variable X_i. The sensitivity coefficients are defined as

$$\theta_i = \frac{\partial r}{\partial X_i} \tag{12}$$

Equation (11) is the desired propagation equation, which was setout to be derived. The equation is used for both single tests and multiple tests as presented next in Section 6.

6. Uncertainty Equations for Single and Multiple Tests

A given set of measurements may be made in several different ways. Ideally, one will be able to repeat the measurements several times. In multiple tests, the result $r = (X_1, X_2, ..., X_J)$ is determined from many sets of measurements $(X_1, X_2, ..., X_J)$ at a fixed test condition with the same measurement systems. However, in some instances (e.g., complex or expensive experiments), it may not be possible to perform a test more than once. For this situation the result $r = (X_1, X_2, ..., X_J)$ is determined from one set of measurements $(X_1, X_2, ..., X_J)$ at a fixed test condition. According to the present methodology, a test is considered a single test if the entire test is performed only once, even if the measurements of one or more of the variables are made from many samples. For example, when measuring the dynamic pressure in a pipe, one may make many samples over a period of time long enough to average out the effects of turbulence. The average of these measurements is taken to be the measurement of that particular variable so that a single value is available.

The total uncertainty in the result, r, for both single and multiple tests is the root-sum-square (RSS) of the bias and precision limits

$$U_r^2 = B_r^2 + P_r^2 \tag{13}$$

The bias limits of the results [B_r in equation (13)] for single and multiple tests are determined in the same manner. The precision limits are determined differently depending upon how the data was collected, i.e., single or multiple test.

6.1. Bias Limits

For both single and multiple tests, the bias limit of the result [B_r in equation (13)] is given by

$$B_r^2 = \sum_{i=1}^{J} \theta_i^2 B_i^2 + 2 \sum_{i=1}^{J-1} \sum_{k=i+1}^{J} \theta_i \theta_k B_{ik} \tag{14}$$

where θ_i are the sensitivity coefficients defined as before

$$\theta_i = \frac{\partial r}{\partial X_i} \tag{15}$$

B_i are the bias limits in X_i and B_{ik} are the correlated bias limits in X_i and X_k

$$B_{ik} = \sum_{\alpha=1}^{L} (B_i)_\alpha (B_k)_\alpha \tag{16}$$

L is the number of correlated bias error sources that are common for measurement of variables X_i and X_k.

The bias limit B_i for each variable is an estimate of elemental bias errors from different categories: calibration errors; data acquisition errors; data reduction errors; and conceptual bias. Within each category, there may be several elemental sources of bias. For instance, if for the ith variable X_i there are J elemental bias errors identified as significant and whose bias limits are estimated as $(B_i)_1$, $(B_i)_2$, . . . , $(B_i)_J$ then the bias limit for the measurement of X_i is calculated as the root-sum-square (RSS) combination of the elemental limits

$$B_i^2 = \sum_{k=1}^{J} (B_i)_k^2 \tag{17}$$

The bias limits for each element $(B_i)_k$ must be estimated for each variable X_i using the best information one has available at the time. In the design phase of an experimental program, manufacturer's specifications, analytical estimates, and previous experience will typically provide the basis for most of the estimates. As the experimental program progresses, equipment is assembled, and calibrations are conducted, these estimates can be updated using the additional information gained about the accuracy of the calibration standards, errors associated with calibration process and curvefit procedures, and perhaps analytical estimates of installation errors (e.g., wall interference effects).

6.2 Precision Limits for Single Tests

For single tests in which one or more of the measurements were made from many samples over some time interval at a fixed test condition, and assuming no correlated precision limits for the precision errors, the precision limit of the result [P_r in equation

(13)] can be estimated by

$$P_r = tS_r \tag{18}$$

where t is the coverage factor and S_r is the standard deviation of the sample of N readings of the result r. For $N \geq 10$ it is assumed that $t = 2$. The value of S_r is determined from N readings over an appropriate/sufficient time interval that includes all factors causing variability in the result.

Alternatively, P_r can be estimated by the RSS of the precision limits for the measurements of the individual variables

$$P_r = \sum_{i=1}^{J} (\theta_i P_i)^2 \tag{19}$$

where θ_i are the sensitivity coefficients defined by equation (15) and $P_i = t_i S_i$ are the precision limits in X_i [where t_i and S_i are defined similarly as t and S_r in equation (18)].

Often it is the case, that the time interval is inappropriate/insufficient and the P_i's or P_r must be estimated based on previous readings (e.g., based on previous multiple tests) or the best available information.

6.3 Precision Limits for Multiple Tests

In multiple tests, an averaged result $\bar{r}$ can also be determined from M sets of measurements $(X_1, X_2, \ldots, X_J)_k$ at the same fixed test condition

$$\bar{r} = \frac{1}{M} \sum_{k=1}^{M} r_k \tag{20}$$

The bias limit of the result B_r is estimated using equation (14). If the M sets of measurements are taken over an appropriate time interval, the precision limit of a single result of the M measurements is

$$P_r = tS_{\bar{r}} \tag{21}$$

where t is determined with M-1 degrees of freedom ($t = 2$ for $M \geq 10$) and $S_{\bar{r}}$ is the standard deviation of the M "sample" distribution of results

$$S_{\bar{r}} = \left[\sum_{k=1}^{M} \frac{(r_k - \bar{r})^2}{M-1} \right]^{1/2} \tag{22}$$

The precision limit for the average result is given by

$$P_{\bar{r}} = \frac{tS_{\bar{r}}}{\sqrt{M}} \tag{23}$$

The total uncertainty for the average result is (using the large sample assumption)

$$U_{\bar{r}}^2 = B_r^2 + P_{\bar{r}}^2 = B_r^2 + \left(2S_{\bar{r}}/\sqrt{M}\right)^2 \tag{24}$$

Alternatively, $P_{\bar{r}}$ can be estimated as the RSS of the precision limits of the individual variables

$$P_{\bar{r}} = \sum_{i=1}^{J} (\theta_i P_{\bar{i}})^2 \tag{25}$$

where the precision limit of one of the measured variables is

$$P_{\bar{i}} = \frac{tS_{\bar{i}}}{\sqrt{M}} \tag{26}$$

and t is taken to be 2 when the number of samples is greater than 10 and S_i is the standard deviation of the M sample results

$$S_{\bar{i}} = \left[\sum_{k=1}^{M} \frac{\left(X_k - \overline{X}_{\bar{i}}\right)^2}{M-1} \right]^{1/2} \tag{27}$$

7. Implementation

The uncertainty assessment methodology is summarized in Figure 1. For each experimental result, the data reduction equation (1) is determined first. Then a block diagram of the test (Figure 3) is constructed to help organize the individual measurement systems and the propagation of elemental error sources into the final result. Data-stream diagrams are constructed next, showing data flow from sensor-to-result and are helpful for identification and organization of the elemental bias and precision limits at the

individual-variable level.

Bias limits contributing either to a single variable or the final result are identified (calibration, data acquisition, data reduction, or conceptual bias) and combined. Once the sources of uncertainty have been identified, their relative significance should be established based on order of magnitude estimates. A "rule of thumb" is that those uncertainty sources that are smaller that 1/4 or 1/5 of the largest sources are usually considered negligible.

For the vast majority of experiments, precision limits are estimated as described above with repeated end-to-end data-acquisition and reduction cycles (i.e., for the final result level as opposed to the individual variable level). Note that the precision limit computed is only applicable for those random error sources that were "active" during the repeated measurements. Ideally $M \geq 10$, however, often this is not the case and for $M < 10$, a coverage factor $t = 2$ is still permissible if the bias and precision limits have similar magnitude. If one encounters unacceptably large P's, the elemental sources' contributions must be examined to see which need to be (or can be) improved.

The precision limit, bias limit, and total uncertainty for the experimental result r are then found. For each experimental result, the bias limit, precision limit, and total uncertainty should be reported.

8. Example for Measurement of Density and Kinematic Viscosity

Professor R. Ettema and Dr. M. Muste developed the present experiment at IIHR during the summer of 1997 for use in the fluids lab. Subsequently, as presented herein, the experiment was revised to include uncertainty assessment. Granger (1988) presents a similar experiment, but without uncertainty assessment.

The experiment determines density and kinematic viscosity of a fluid by equating forces on a sphere falling at terminal velocity and low Reynolds number (Roberson and Crowe, 1997, pp. 438-443). More commonly, density is determined from specific weight measurements using hydrometers (Roberson and Crowe, 1997, pg. 57) and viscosity is determined using capillary viscometers.

The purpose of the experiment is to provide a relatively simple, yet comprehensive, tabletop measurement system for demonstrating fluid mechanics

concepts, experimental procedures, and uncertainty assessment. The measurements are compared with benchmark data based both on reference data provided by the fluid (99.7% aqueous glycerin solution) manufacturer and measurements using a commercially available hydrometer and capillary viscometer.

8.1. Test Design

A sphere of diameter D falls at terminal velocity V through a long transparent cylinder filled with fluid of density ρ, viscosity μ, and kinematic viscosity ν (= μ/ρ), as shown in Figure 7. The acceleration is zero, hence, the forces acting on the sphere must sum to zero. These forces of gravity F_g, buoyancy F_b, and drag F_d, sum as:

$$W_a = F_g - F_b = F_d \tag{28}$$

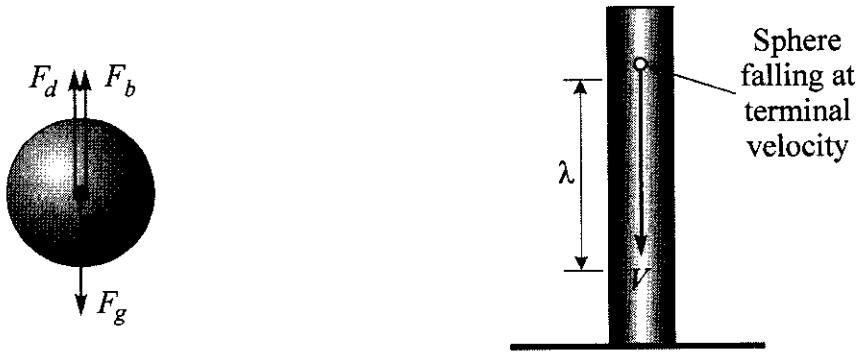

Figure 7. Experimental arrangement

The apparent weight is given by

$$W_a = \gamma \nabla (S - 1) \tag{29}$$

where $\gamma = \rho g$ is the specific weight of the fluid, $\nabla = \pi D^3/6$ is the volume of the sphere, and $S = \rho_{sphere}/\rho$ is the specific gravity of the sphere. For very low Reynolds number $Re = VD/\nu << 1$, the drag force F_d is approximated by Stokes law (White, 1994, pp. 173-178)

$$F_d = 3\pi\mu VD \tag{30}$$

Although strictly valid only for $Re << 1$, Stokes law agrees with experiments up to $Re < 1$. For $Re > 1$, the wake becomes asymmetric, and for $Re > 20$, the flow separates and pressure drag increases significantly. Substituting equations (29) and (30) into equation (28) and solving for V results in

$$V = \frac{gD^2}{18\nu}(S-1) \tag{31}$$

Equation (31) shows that the terminal velocity (for $Re << 1$) is proportional to both D^2 and (S-1) and inversely proportional to ν. The terminal velocity can equivalently be expressed by $V = \lambda/t$ where λ and t are the fall distance and time, respectively. λ is labeled in Figure 7. Alternatively, solving for ν and substituting λ/t for V results in

$$\nu = \nu(D,t,\lambda,\rho) = \frac{gD^2t}{18\lambda}(S-1) \tag{32}$$

Evaluating equation (32) for two different spheres (e.g., teflon and steel, as indicated by subscripts t and s), equating, and solving for ρ results in

$$\rho = \rho(D_t,t_t,D_s,t_s) = \frac{D_t^2 t_t \rho_t - D_s^2 t_s \rho_s}{D_t^2 t_t - D_s^2 t_s} \tag{33}$$

Equations (32) and (33) are data-reduction equations for $\nu=\nu_t=\nu_s$ and ρ in terms of measurements of individual variables: D_t, D_s, t_t, t_s, and λ.

8.2. Measurement Systems and Procedures

Figure 8 provides a block diagram of the experiment indicating the individual measurement systems, data reduction equations and results, and propagation of errors. The individual measurement systems are for the sphere diameters D_t and D_s, fall distance λ, and fall times t_t and t_s. The sphere diameters are measured with a micrometer of resolution 0.01mm. The fall distance is measured with a scale of resolution 1/16 inch. The fall times are measured with a stopwatch with last significant digit 0.01 sec.

Teflon and steel spheres are used for the experiments. The sphere densities are assumed constant, as provided by the manufacturer (Small Part Inc., 1998). These values along with that used for the gravitational acceleration are provided in Table 1. The fluid

used for the experiments is 99.7% aqueous glycerin solution. The manufacturer (Proctor&Gamble, 1995) provided reference data for density and kinematic viscosity, as a function of ambient temperature. To enable the comparison between the present measurements and the manufacturer values, temperature was also measured with a digital thermometer with last significant digit 0.1°F. Uncertainties for the manufacturer values and temperature measurement were not considered.

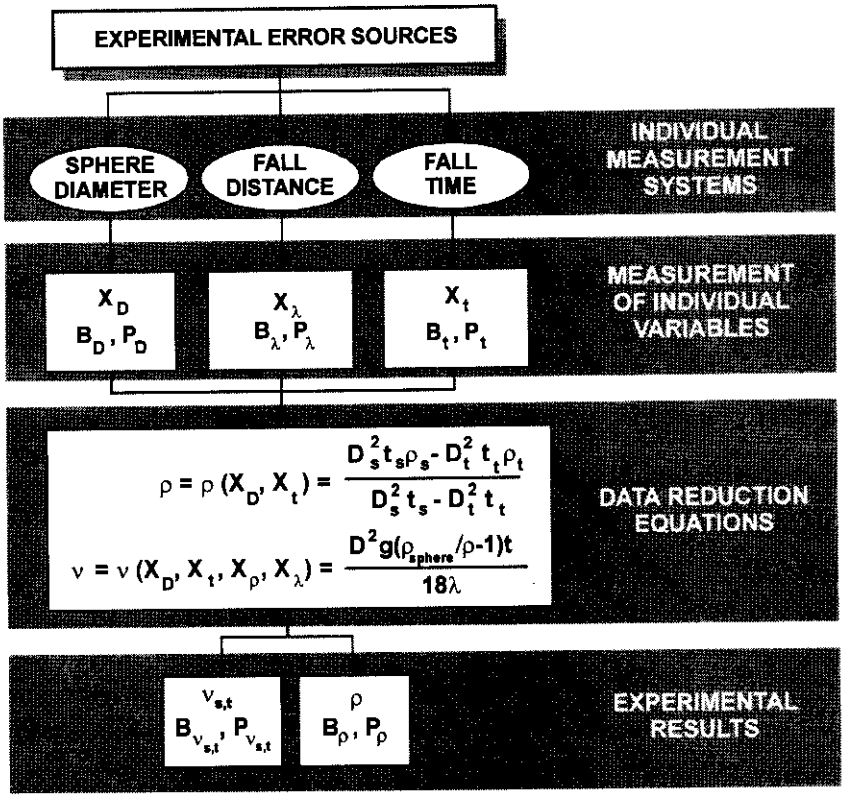

Figure 8. Block diagram of experiment

The data acquisition procedure consists of three steps: (1) measure the ambient temperature T and fall distance λ; (2) measure diameters D_t and fall times t_t for 10 teflon spheres; and (3) measure diameters D_s and fall times t_s for 10 steel spheres. Care should be taken in coordination of the starting and stopping of the stopwatch with the sphere crossings of the upper and lower fall distance markings, as shown in Figure 7. Data reduction is done at steps (2) and (3) by substituting the measurements for each test into the data reduction equation (33) for evaluation of ρ and then along with this result into the data reduction equation (32) for evaluation of ν.

Table 1. Gravity and sphere density constants

Definitions	Symbol	Value
Gravitational acceleration	g	9.81 m/s^2
Density of steel	ρ_s	7991 kg/m^3
Density of teflon	ρ_t	2148 kg/m^3

8.3. Test Results

Typical test results are provided in Table 2. The results include measurements of temperature T and fall distance λ along with measurements taken 10 times repeatedly for teflon and steel sphere diameters and fall times (D_t, t_t, D_s, t_s), fluid density ρ, and kinematic viscosity ν. Also shown are the average values and standard deviations. These values will be used and explained in conjunction with the uncertainty assessment. Using the averaged values for V, D, and ν, $Re_t = 0.18$ and $Re_s = 0.26$ both of which meet the requirement $Re < 1$.

Table 2. Typical test results

Trial	**TEFLON**		**STEEL**		**RESULTS**	
T= 26.4 °C	D_t	t_t	D_s	t_s	ρ	ν
λ = 0.61 m	(m)	(sec)	(m)	(sec)	(kg/m^3)	(m^2/s)
1	0.00661	31.08	0.00359	12.210	1382.14	0.000672
2	0.00646	31.06	0.00358	12.140	1350.94	0.000683
3	0.00634	30.71	0.00359	12.070	1305.50	0.000712
4	0.00632	30.75	0.00359	12.020	1304.66	0.000709
5	0.00634	30.89	0.00359	12.180	1302.38	0.000720
6	0.00633	30.82	0.00359	12.060	1306.70	0.000710
7	0.00637	30.89	0.00359	12.110	1317.75	0.000710
8	0.00634	30.71	0.00359	12.120	1301.50	0.000717
9	0.00633	31.2	0.00359	12.030	1320.75	0.000700
10	0.00634	31.11	0.00359	12.200	1307.64	0.000718
Average	0.006375	30.91	0.003589	12.114	1318.80	0.000706
Std.Dev. (S_i)	$9.17 \cdot 10^{-5}$	0.18	$3.16 \cdot 10^{-6}$	0.0687	26.74	$1.597 \cdot 10^{-5}$

8.4. Uncertainty Assessment

Uncertainties are estimated for the experimental results for density ρ and kinematic viscosity ν. The estimates are done using both multiple and single test methods. The B_i's are estimated at the individual variable level and evaluated for the

results using the propagation equation (14). For ρ, results are presented both without and with including the correlated bias errors. The P_r's are estimated at the end-to-end level. For multiple tests, $P_{\bar{r}}$ is given by equation (23) with the standard deviation S_r evaluated using equation (22) for the 10 repeated tests. For the single test, P_r is given by equation (18) with S_r estimated from the multiple test results. For comparison, P_r's estimated by RSS of the individual variables are provided in Appendix A (for the multiple test method). Details are given for estimating U_ρ and U_{v_t} using the multiple test method. The estimates for U_{v_s} using the multiple test method and the estimates for the single test method are also mentioned.

8.4.1 Multiple Tests

Density ρ. The data reduction equation for density is given by equation (33). The total uncertainty for the average density is given by equation (24) with $r = \rho$

$$U_{\bar{\rho}}^2 = B_\rho^2 + \left(2S_{\bar{\rho}}/\sqrt{M}\right)^2 \tag{34}$$

and M=10 (the number of repeat tests).

Bias limits. The bias limit in equation (34) is given by equation (14)

$$B_\rho^2 = \theta_{D_t}^2 B_{D_t}^2 + \theta_{t_t}^2 B_{t_t}^2 + \theta_{D_s}^2 B_{D_s}^2 + \theta_{t_s}^2 B_{t_s}^2 + 2\theta_{D_t}\theta_{D_s} B_{D_t} B_{D_s} + 2\theta_{t_t}\theta_{t_s} B_{t_t} B_{t_s} \tag{35}$$

B_i are the bias limits for the individual variables (D_t, D_s, t_t, t_s) and $\theta_i = \partial r/\partial X_i$ are the sensitivity coefficients. Note that the bias limits for D_t and D_s as well as t_t and t_s are correlated because the sphere diameters and fall times are measured with the same instrumentation. The bias limits for the individual variables are based on the resolution of the instruments (micrometer and stopwatch) used to make the measurements. A summary of the bias limits for individual variables, their relative magnitude to the average values, and the source/method of their estimation are provided in Table 3.

Table 3. Bias limits for individual variables D and t

Bias Limit	Magnitude	Percentage Values	Estimation
$B_D = B_{D_t} = B_{D_S}$	0.000005 m	0.078 % D_t 0.14 % D_s	½ instrument resolution
$B_t = B_{t_t} = B_{t_t}$	0.01 s	0.032% t_t 0.083% t_s	Last significant digit

The sensitivity coefficients are evaluated using the average values for the individual variables from Table 2

$$\theta_{D_t} = \frac{\partial \rho}{\partial D_t} = \frac{2\, D_s^2\, t_t\, t_S\, D_t (\rho_S - \rho_t)}{\left[D_t^2\, t_t - D_s^2\, t_S\right]^2} = 296{,}808\, \frac{kg}{m^4} \qquad \theta_{t_t} = \frac{\partial \rho}{\partial t_t} = \frac{D_s^2 D_t^2\, t_S (\rho_S - \rho_t)}{\left[D_t^2\, t_t - D_s^2\, t_s\right]^2} = 30.60\, \frac{kg}{m^3 \cdot s}$$

$$\theta_{D_t} = \frac{\partial \rho}{\partial D_s} = \frac{2\, D_t^2\, t_t\, t_S\, D_S (\rho_t - \rho_S)}{\left[D_t^2\, t_t - D_s^2\, t_S\right]^2} = -527{,}208\, \frac{kg}{m^4} \qquad \theta_{t_t} = \frac{\partial \rho}{\partial t_s} = \frac{D_s^2 D_t^2\, t_t (\rho_t - \rho_S)}{\left[D_t^2\, t_t - D_s^2\, t_s\right]^2} = -78.1\, \frac{kg}{m^3 \cdot s}$$

The total bias limit for density of glycerin is obtained by combining the bias estimates from Table 3 with the above calculated sensitivity coefficients in equation (35) and at first neglecting the last two terms corresponding to the correlated bias errors. The total bias limit as well as its components are shown in Table 4. $B_\rho = 3.13$ kg/m^3 is 0.24% of the measured average density ($\overline{\rho} = 1318.80$ kg/m^3). The contribution of the $\theta_i B_i$'s to B_ρ is small (i.e., less than 1/4 or 1/5 of the $\theta_D B_D$'s); therefore, can be neglected. Although the individual variable biases themselves are small (Table 3), it's their combination with the appropriate sensitivity coefficient that determines their relative contribution to B_ρ.

If the terms corresponding to the correlated bias errors in equation (35) are considered, the total bias limit is decreased, as shown in Table 4. $B_\rho = 1.22$ kg/m^3 is 0.09% of $\overline{\rho}$. Note that the consideration of the correlated bias errors has a favorable effect on the total bias limit due to the fact that these terms have negative signs in equation (35) due to the product vs. square of the sensitivity coefficients.

Precision limits. $P_{\overline{\rho}}$ is given by equation (23) with the standard deviation $S_{\overline{\rho}}$ evaluated using equation (22) for the 10 repeat tests, i.e., $S_{\overline{\rho}} = 26.74$ kg/m^3 (Table 2)

$$P_{\overline{\rho}} = \frac{2 \cdot S_{\overline{\rho}}}{\sqrt{M}} = \frac{2 \cdot 26.74}{\sqrt{10}} = 16.91\ \frac{kg}{m^3}$$

$P_{\bar{\rho}}$ is 1.28% of the measured average density, as shown in Table 4.

Total uncertainty. The total uncertainty for density is evaluated from equation (34). If the correlated bias errors are neglected

$$U_{\bar{\rho}} = \pm\sqrt{B_{\rho}^2 + P_{\bar{\rho}}^2} = \pm\sqrt{3.13^2 + 16.91^2} = \pm 17.20\ kg/m^3,$$

otherwise,

$$U_{\bar{\rho}} = \pm\sqrt{B_{\rho}^2 + P_{\bar{\rho}}^2} = \pm\sqrt{1.22^2 + 16.91^2} = \pm 16.95\ kg/m^3$$

$U_{\bar{\rho}}$ estimated without considering the correlated bias errors is 1.3% of the measured average density, as shown in Table 4. 97% of the total uncertainty is due to the precision limit, whereas only 3% is due to the bias limit. $U_{\bar{\rho}}$ accounting for correlated bias errors is 1.28% of the measured average density, as shown in Table 4. 99.5% of the total uncertainty is due to the precision limit, whereas only 0.5% is due to the bias limit, which is the reason the effects of the correlated bias errors have a large effect on the bias limit and a minimal effect on the total uncertainty.

Table 4. Uncertainty estimates for density using multiple test method

Term	Without correlated bias errors		With correlated bias errors	
	Magnitude	Percentage Values	Magnitude	Percentage Values
$\theta_{D_t} B_D$	1.48 kg/m^3	22.30% B_{ρ}^2	1.48 kg/m^3	147.16% B_{ρ}^2
$\theta_{t_t} B_t$	0.31 kg/m^3	0.95% B_{ρ}^2	0.31 kg/m^3	4.09% B_{ρ}^2
$\theta_{D_s} B_D$	-2.63 kg/m^3	70.60% B_{ρ}^2	-2.63 kg/m^3	464.72% B_{ρ}^2
$\theta_{t_s} B_t$	-0.78 kg/m^3	6.15% B_{ρ}^2	-0.78 kg/m^3	38.89% B_{ρ}^2
$2\theta_{D_t}\theta_{D_s} B_D^2$	-	-	-2.79 kg/m^3	-522.98% B_{ρ}^2
$2\theta_{t_t}\theta_{t_s} B_t^2$	-	-	-0.69 kg/m^3	-31.88% B_{ρ}^2
B_{ρ}	3.13 kg/m^3	0.24% $\bar{\rho}$ 3.3% $U_{\bar{\rho}}^2$	1.22 kg/m^3	0.09% $\bar{\rho}$ 0.47% $U_{\bar{\rho}}^2$
$P_{\bar{\rho}}$	16.91 kg/m^3	1.28% $\bar{\rho}$ 96.70% $U_{\bar{\rho}}^2$	16.91 kg/m^3	1.29% $\bar{\rho}$ 99.53% $U_{\bar{\rho}}^2$
$U_{\bar{\rho}}$	17.20kg/m^3	1.30% $\bar{\rho}$	16.95kg/m^3	1.28% $\bar{\rho}$

Kinematic viscosity ν_t. The data reduction equation is given by equation (32). The total uncertainty for the average kinematic viscosity is given by equation (24) with $r = \nu_t$

$$U_{\bar{\nu}_t}^2 = B_{\nu_t}^2 + \left(2S_{\bar{\nu}_t}/\sqrt{M}\right)^2 \tag{36}$$

and M=10 (the number of repeat tests).

Bias limits. The bias limit in equation (36) is given by equation (14)

$$B_{\nu_t}^2 = \theta_{D_t}^2 B_D^2 + \theta_\rho^2 B_\rho^2 + \theta_{t_t}^2 B_t^2 + \theta_\lambda^2 B_\lambda^2 \tag{37}$$

Note that there are no correlated bias errors contributing to the viscosity result. The bias limits B_D, B_ρ, and B_t were evaluated in conjunction with estimation of $U_{\bar{\rho}}$. The bias limit B_λ is based on the resolution of the scale used in making the measurement, as shown in Table 5. The sensitivity coefficients are evaluated using the average values for the individual variables and result for ρ from Table 2

$$\theta_{D_t} = \frac{\partial \nu}{\partial D_t} = \frac{2D_t g(\rho_t/\rho - 1)t_t}{18\lambda} = 0.202 \quad \frac{m}{s} \qquad \theta_\rho = \frac{\partial \nu}{\partial \rho} = \frac{D_t^2 g \rho_t t_t}{18\lambda\rho^2} = 1.36\times10^{-6} \frac{m^5}{kg\cdot s}$$

$$\theta_{t_t} = \frac{\partial \nu}{\partial t} = \frac{D_t^2 g(\rho_t/\rho - 1)}{18\lambda} = 2.27x10^{-5} \quad \frac{m^2}{s^2} \qquad \theta_\lambda = \frac{\partial \nu}{\partial \lambda} = -\frac{D_t^2 g(\rho_t/\rho - 1)t_t}{18\lambda^2} = -1.15x10^{-3} \quad \frac{m}{s}$$

Combining the bias estimates from Tables 3 and 5 with the sensitivity coefficients given above into equation (37) provides values for the total bias limit as well as its components, as shown in Table 5. $B_{\nu_t} = 4.5\times10^{-6}$ m^2/s is 0.64% of the measured average kinematic viscosity ($\bar{\nu}_t$ = 0.000707 m^2/s). The major contribution to the bias limit of the kinematic viscosity is $\theta_\rho B_\rho$; therefore, the others can be neglected.

Precision limits. $P_{\bar{r}}$ is given by equation (23) with the standard deviation $S_{\bar{r}}$ evaluated using equation (22) for the 10 repeated tests, i.e., $S_{\bar{\nu}_t} = 1.6\times10^{-5}$ m^2/s (Table 2)

$$P_{\bar{\nu}_t} = \frac{2\cdot S_{\bar{\nu}_t}}{\sqrt{M}} = \frac{2\cdot 1.6\cdot 10^{-5}}{\sqrt{10}} = 1.01\cdot10^{-5}\frac{m^2}{s}$$

$P_{\bar{\nu}_t}$ 1.43% of the measured average kinematic viscosity, as shown in Table 5.

Total uncertainty. The total uncertainty for kinematic viscosity is evaluated from equation (36)

$$U_{\bar{\nu}_t} = \pm\sqrt{(4.5\cdot10^{-6})^2 + (1.01\cdot10^{-5})^2} = \pm1.11\cdot10^{-5}\, m^2/s$$

$U_{\bar{\nu}_t}$ is 1.57% of the measured average kinematic viscosity, as shown in Table 5. 84% of the total uncertainty is due to the precision limit, whereas 16% is due to the bias limit.

Kinematic viscosity ν_s. Uncertainty estimates were also obtained for the kinematic viscosity using the measurements for the steel spheres following exactly the same procedure previously described for the teflon spheres. The total uncertainty is $U_{\bar{\nu}_s}$ = ± 1.49% of the measured average kinematic viscosity, which is nearly the same as that for the teflon spheres.

Table 5. Uncertainty estimates for kinematic viscosity (teflon spheres) using multiple test method

Term	Magnitude	Percentage Values
B_λ	7.9×10^{-4} m	0.13% λ
$\theta_{D_t} B_D$	1.1×10^{-6} m^2/s	5.97% $B^2_{\nu_t}$
$\theta_\rho B_\rho$	4.27×10^{-6} m^2/s	90.03% $B^2_{\nu_t}$
$\theta_{t_t} B_t$	2.29×10^{-7} m^2/s	0.26% $B^2_{\nu_t}$
$\theta_\lambda B_\lambda$	-0.92×10^{-6} m^2/s	3.74% $B^2_{\nu_t}$
B_{ν_t}	4.5×10^{-6} m^2/s	0.64% $\overline{\nu_t}$ 16.43% $U^2_{\bar{\nu}_t}$
$P_{\bar{\nu}_t}$	1.01×10^{-5} m^2/s	1.43% $\overline{\nu_t}$ 83.57% $U^2_{\bar{\nu}_t}$
$U_{\bar{\nu}_t}$	1.11×10^{-5} m^2/s	1.57% $\overline{\nu_t}$

8.4.2. Single Test

Uncertainty estimates for a single test are made using the measurements for trial 7 of the repeated tests, as provided in Table 2. The precision limit is estimated for the single test using the standard deviation for the multiple test as a best estimate.

Density ρ. The total uncertainty is given by equation (13)

$$U_\rho^2 = B_\rho^2 + P_\rho^2 \tag{38}$$

Bias limits. The bias limit is given by equation (35) evaluated using the same B_i's as for the multiple tests, but with the sensitivity coefficients evaluated using the single test values. Table 6 includes the estimates for bias limit and its components without and with considering the contribution of the correlated bias errors. As shown in Table 6, the results are nearly the same as for the multiple test method since the only difference is in evaluating the sensitivity coefficients using trial 7 values instead of the average values. Similarly to the multiple tests case, consideration of the correlated bias errors has a favorable effect on the total bias limit, decreasing the magnitude of the bias limit and the total uncertainty as well.

Precision limits. P_r is given by equation (18) with S_r estimated from the multiple test results, i.e., is $S_\rho = 26.74$ kg/m^3 (Table 2)

$$P_\rho = tS_\rho = 53.47 \text{ kg/m}^3 \tag{39}$$

and $t = 2$. P_ρ is 4.05% of the measured average density, as shown in Table 6. P_r for the single test is $\sqrt{M} = 3.16$ larger than $P_{\bar{\rho}}$ for the multiple tests.

Total uncertainties. The total uncertainty for density using the single test method is evaluated from equation (38). If the correlated bias errors are neglected

$$U_\rho = \pm\sqrt{3.14^2 + 53.48^2} = \pm 53.56 \; kg/m^3$$

Otherwise,

$$U_\rho = \pm\sqrt{1.23^2 + 53.48^2} = \pm 53.50 \; kg/m^3$$

U_ρ estimated without considering the correlated bias errors is 4.06% of the measured average density, as shown in Table 6. 99.65% of the total uncertainty is due to the precision limit, whereas 0.35% is due to the bias limit. The single test method bias limit is nearly the same and the precision limit is larger than that for the multiple tests; thereby, increasing the total uncertainty. U_ρ accounting for the correlated bias errors is 4.05% of the measured average density, as shown in Table 6. 99.89% of the total uncertainty is due to the precision limit, whereas 0.11% is due to the bias limit.

Table 6. Uncertainty estimates for density using single test method

Term	Without correlated bias errors		With correlated bias errors	
	Magnitude	Percentage Values	Magnitude	Percentage Values
$\theta_{D_t} B_D$	1.49 kg/m^3	22.60% B_ρ^2	1.49 kg/m^3	147.74% B_ρ^2
$\theta_{t_t} B_t$	0.31 kg/m^3	0.96% B_ρ^2	0.31 kg/m^3	4.01% B_ρ^2
$\theta_{D_s} B_D$	-2.64 kg/m^3	70.70% B_ρ^2	-2.64 kg/m^3	462.68% B_ρ^2
$\theta_{t_s} B_t$	-0.78 kg/m^3	5.74% B_ρ^2	-0.78 kg/m^3	38.70% B_ρ^2
$2\theta_{D_t}\theta_{D_s} B_D^2$	-	-	-2.81 kg/m^3	-522.95% B_ρ^2
$2\theta_{t_t}\theta_{t_s} B_t^2$	-	-	-0.69 kg/m^3	-30.18% B_ρ^2
B_ρ	3.14 kg/m^3	0.24% ρ 0.35% U_ρ^2	1.23 kg/m^3	0.09% ρ 0.11% U_ρ^2
P_ρ	53.47 kg/m^3	4.05% ρ 99.65% U_ρ^2	53.47 kg/m^3	4.05% ρ 99.89% U_ρ^2
U_ρ	53.56 kg/m^3	4.06% ρ	53.50 kg/m^3	4.05% ρ

Kinematic viscosity ν_t and ν_s. Uncertainty estimates were also obtained for the kinematic viscosity using the single test method for both the teflon and steel spheres. The procedures closely followed those just described for the single test method for estimating the density U_ρ. Table 7 shows the detailed results for the teflon spheres. The total uncertainty for the kinematic viscosity for steel spheres is $U_{\nu_s} = \pm 5.03\%$ of the measured average kinematic viscosity.

Table 7. Uncertainty estimates for kinematic viscosity (teflon spheres) using single test method

Term	Magnitude	Percentage Values
$\theta_{D_t} B_D$	1.1×10^{-6} m^2/s	5.82% $B_{\nu_t}^2$
$\theta_\rho B_\rho$	4.36×10^{-6} m^2/s	89.84% $B_{\nu_t}^2$
$\theta_{t_t} B_t$	2.3×10^{-7} m^2/s	0.25% $B_{\nu_t}^2$
$\theta_\lambda B_\lambda$	-0.9×10^{-6} m^2/s	3.99% $B_{\nu_t}^2$
B_{ν_t}	4.6×10^{-6} m^2/s	0.65% ν_t 1.85% $U_{\nu_t}^2$
P_{ν_t}	3.2×10^{-5} m^2/s	4.53% ν_t 98.15% $U_{\nu_t}^2$
U_{ν_t}	3.23×10^{-5} m^2/s	4.55% ν_t

8.5. Discussion of Results

Test results for density ρ and kinematic viscosity ν of glycerin were obtained at four temperatures between 26-29°C, as shown in Figures 9 and 10. The uncertainty estimates without correlated bias errors are shown as uncertainty bands. Note that the uncertainty estimates are for T = 26.4° C, but are assumed applicable for all T. Table 8 summarizes the total uncertainty estimates for ρ and both ν_t and ν_s.

The values and trends for ρ and ν seem reasonable in comparison to textbook values, e.g., Roberson and Crow (1997, pg. A-23), although the measured ν value is larger than the textbook value. The textbook only provides values at 20°C (and atmospheric pressure) of ρ= 1260 kg/m^3 and ν= 0.00051 m^2/s. The uncertainty estimates also seem reasonable and are relatively small, especially for the multiple tests (i.e., < 2% of the measured average values).

Table 8. Total uncertainty estimates for density and kinematic viscosity of glycerin (values in parenthesis include consideration of correlated bias errors)

Assessment Method	U_ρ	U_ν	
		Teflon Spheres	Steel Spheres
Single Test	± 4.06 (4.05)% $\bar{\rho}$	± 4.55 % $\bar{\nu}$	± 5.03 % $\bar{\nu}$
Multiple Tests (M = 10)	± 1.30 (1.28)% $\bar{\rho}$	± 1.57 % $\bar{\nu}$	± 1.49 % $\bar{\nu}$

The ratio of the measured fall times for the teflon and steel spheres is t_t/t_s=2.55, as provided by the Table 2 test results, which is about 27.5% larger than that calculated from equation (29).

8.6 Comparison with Benchmark Data

Validation of the test procedures and data requires known benchmark values B and uncertainties U_B at the correct temperature (and pressure). A comparison error $E = D - B$ (where D represents the present data) and uncertainty $U_E^2 = U_D^2 + U_B^2$ (where U_D represents the present data uncertainties) can be defined. The condition for validation of an experiment against a benchmark is that $|E| \le U_E$, whereupon it can be stated that the experimental procedures and data have been validated at the U_E level. In other words,

the differences between the test procedure and data and the benchmark is within the "noise level" of the comparison.

The present measurements are compared with benchmark data based both on reference data provided by the glycerin manufacturer and measurements using a commercially available hydrometer and capillary viscometer. Unfortunately, as discussed next, a complete validation is not possible since U_B is unknown for the reference data and is uncertain for the hydrometer and capillary viscometer. Moreover, the reference data does not include the effects of solution concentration of glycerin. However, E and U_D can evaluated and compared.

Reference data was solicited from the manufacturer of the glycerin (Proctor & Gamble, 1995). Reference data was provided based on available literature for 100% glycerin as a function of ambient temperature (and for standard atmospheric pressure). Uncertainty estimates for the reference data are not available. The effects of solution concentration or correction/extrapolation procedures are not known, i.e., differences for 99.7% aqueous glycerin solution vs. the 100% glycerin.

An ErTco hydrometer was used to measure the specific weight of a sample of the 99.7% aqueous glycerin solution (used in the experiments), which was converted to density ρ using the g = 9.81 m/s^2 (Table 1). The resolution of the hydrometer is 10 kg/m^3. Similarly, a Cannon glass capillary viscometer was used to measure the kinematic viscosity. The resolution of the capillary viscometer is 4.32×10^{-6} m^2/s. The manufacturers provide certificates of calibration in accordance with National Institute of Standards and Technology. For the capillary viscometer, the uncertainty relative to the primary standard is quoted at ± 0.45% of the measured kinematic viscosity for the present conditions. Presumably, U_B is small for both instruments (< 1%), but we are reluctant to state a value for U_B without confirmation, especially for the capillary viscometer which involves a somewhat more complex measurement procedure than that for the hydrometer.

Figure 9 includes a comparison between the measured densities and the benchmark data and textbook value. The comparison error (using the values at 26.4 °C) for both single and multiple tests is E = 4.9% for the reference data and E = 5.4% for the ErTco hydrometer. The two benchmark data and the textbook value are in close

agreement, i.e., differ by <1%. The comparison uncertainty is $U_E \approx U_D = 4.06\%$ for the single test and $U_E \approx U_D = 1.30\%$ for the multiple tests (neglecting correlated bias errors) since U_B values are not known, but presumably small. The test results are not validated since $|E| \geq U_E$. The fact that E is nearly constant suggests the presence of an unaccounted bias error.

Figure 10 includes a similar comparison for the measured kinematic viscosity and the benchmark data and textbook value. The comparison error (using the values at 26.4 °C) both for single and multiple tests and teflon and steel spheres is about $E = 3.95\%$ for the reference data and $E = 40.6\%$ for the Cannon capillary viscometer. In this case, the two benchmark data and textbook values are not in close agreement, i.e., differ by about 35%. The comparison uncertainty for the teflon spheres is $U_E \approx U_D = 4.55\%$ for the single test and $U_E \approx U_D = 1.57\%$ for the multiple tests, whereas for the steel spheres is $U_E \approx U_D = 5.03\%$ for the single test and $U_E \approx U_D = 1.49\%$ for the multiple tests (neglecting correlated bias errors). Thus, for the reference data, the test results for the single test are validated at about the 5% level, whereas the test results for the multiple tests are not validated. The test results are not validated for the Cannon capillary viscometer. Here again, the fact that E is nearly constant suggests the presence of an unaccounted bias error. Future work should explain the unaccounted bias errors for both ρ and ν and for the differences between the benchmark data and textbook values for ν.

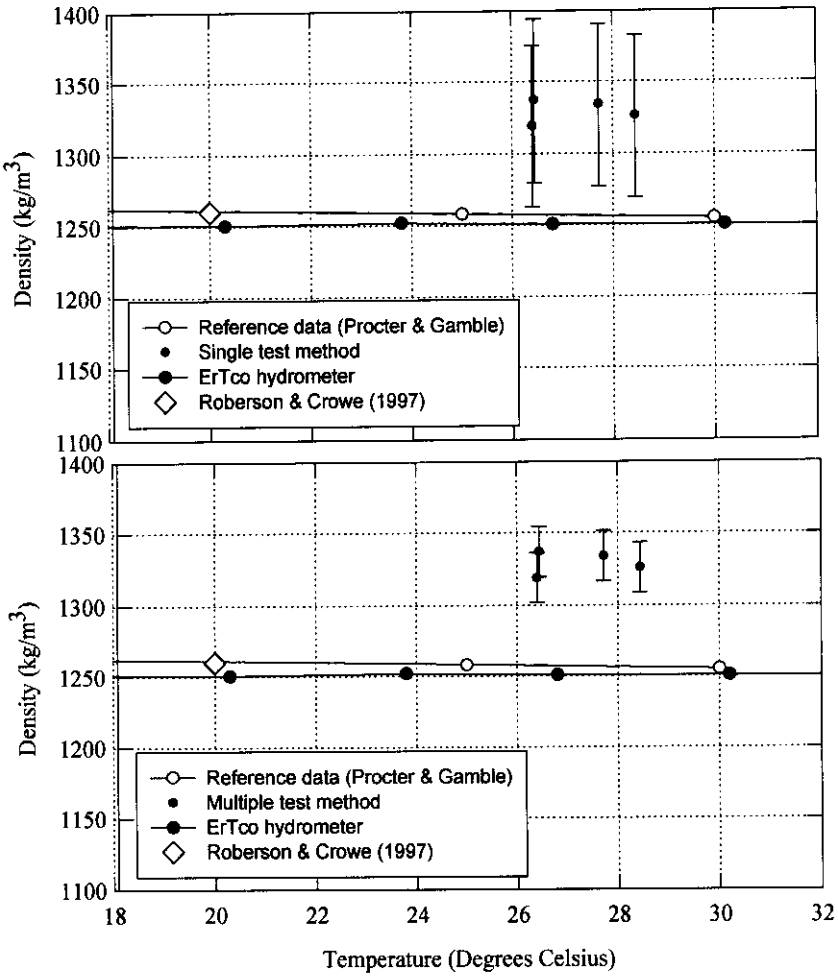

Figure 9. Density of 99.7% aqueous glycerin solution test results and comparison with benchmark data

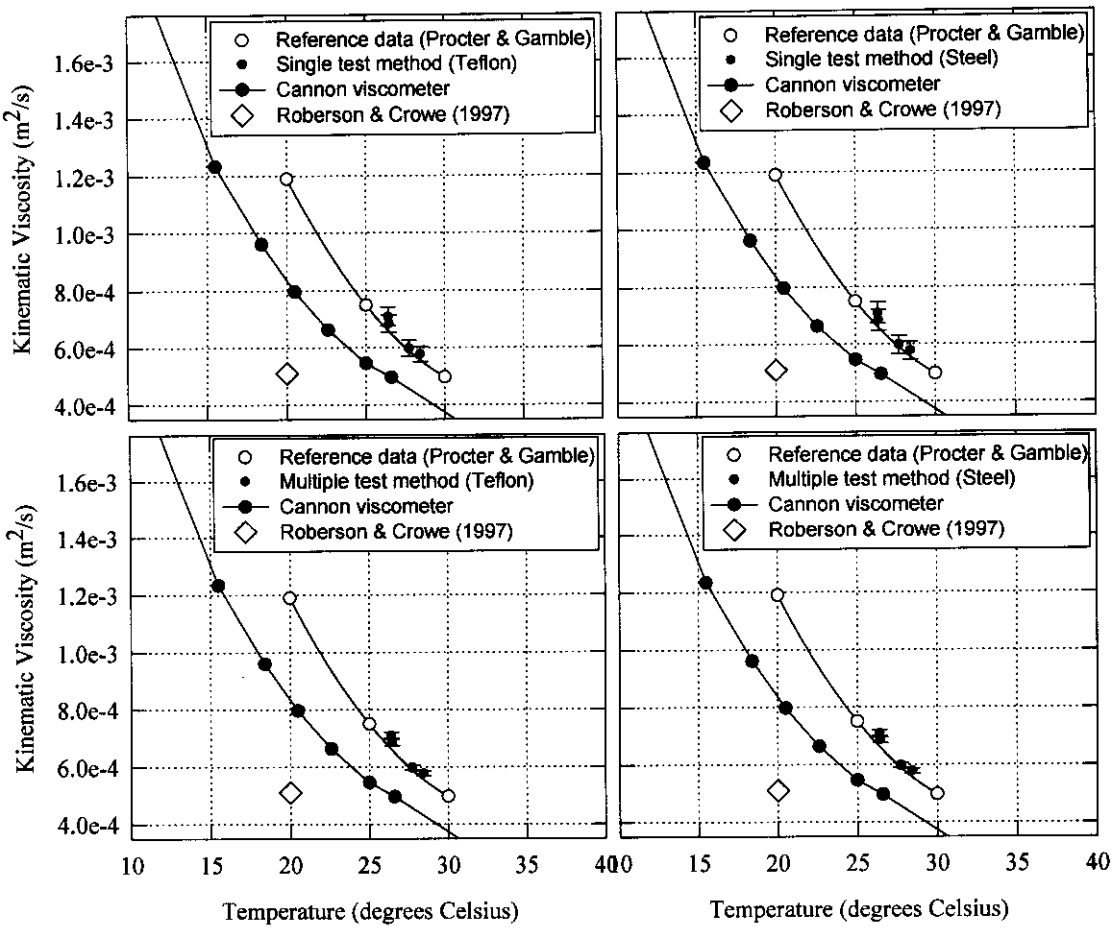

Figure 10. Kinematic viscosity of 99.7% aqueous glycerin solution test results and comparison with benchmark data

9. Conclusions and Recommendations

The AIAA Standard (1995) for experimental uncertainty assessment methodology with associated philosophy of testing is relatively easy to integrate into the overall test process, as demonstrated by the present simple tabletop experiment. The authors firmly believe that the benefits of uncertainty assessment (insurance of uncertainty interval within which true value will lie with a chosen confidence) in reducing risk far outweigh any actual or perceived time saved in foregoing making estimates. Furthermore, as is

often the case (including the present example as well as most of the other fluids laboratory experiments) integration of uncertainty assessment is required for debugging of the test design to obtain satisfactory results.

Recommendations for application/integration of uncertainty assessment methodology by students and faculty are as follows:

1. Recognition that uncertainty depends on entire testing process and that any changes in the process can significantly affect the uncertainty of the test results
2. Full integration of uncertainty assessment methodology into all phases of the testing process including design, planning, calibration, execution and post-test analyses
3. Simplified analyses by using prior knowledge (e.g., data base), tempered with engineering judgement and with effort concentrated on dominant error sources and use of end-to-end calibrations and/or bias and precision limit estimation
4. Documentation, including
   a. test design, measurement systems, and data streams in block diagrams
   b. equipment and procedures used
   c. error sources considered
   d. all estimates for bias and precision limits and the methods used in their estimation (e.g., manufacturers specifications, comparisons against standards, experience, etc.)
   e. detailed uncertainty assessment methodology and actual data uncertainty estimates

Recommendations for administrators of academic laboratories and facilities are as follows:

1. Commitment to full implementation, including provision of adequate resources
2. Provision of proper initial and continued training for responsible test engineers
3. Facilitate application/integration through development of appropriate handbooks and databases
4. Informing students and customers of the uncertainty assessment methodology used and which uncertainties that can be expected for each type of tests

References

AIAA, 1995, "Assessment of Wind Tunnel Data Uncertainty," AIAA S-071-1995.

ANSI/ASME, 1985, "Measurement Uncertainty: Part 1, Instrument and Apparatus," ANSI/ASME PTC 19.I-1985.

Coleman, H.W. and Steele, W.G., 1999, Experimentation and Uncertainty Analysis for Engineers, 2nd Edition, John Wiley & Sons, Inc., New York, NY.

Coleman, H.W. and Steele, W.G., 1995, "Engineering Application of Experimental Uncertainty Analysis," AIAA Journal, Vol. 33, No.10, pp. 1888 – 1896.

Granger, R.A., 1988, Experiments in Fluid Mechanics, Holt, Rinehart and Winston, Inc., New York, NY.

ISO, 1993, "*Guide to the Expression of Uncertainty in Measurement*,", 1st edition, ISBN 92-67-10188-9.

ITTC, 1999, Proceedings 22nd International Towing Tank Conference, "Resistance Committee Report," Seoul Korea and Shanghai China.

Proctor&Gamble, 1995, private communication.

Roberson, J.A. and Crowe, C.T., 1997, Engineering Fluid Mechanics, 6th Edition, Houghton Mifflin Company, Boston, MA.

Small Part Inc., 1998, Product Catalog, Miami Lakes, FL.

White, F.M., 1994, Fluid Mechanics, 3rd edition, McGraw-Hill, Inc., New York, NY.

Apenndix A. Individual Variable Precision Limit

The precision limits presented in sections 8.4.1 and 8.4.2 were estimated using repeated end-to-end data-acquisition and reduction cycles. An alternative procedure for estimation of precision limits is presented herein, where the precision limits are calculated using the RSS of the precision limits for the measurements of the individual variables. Results are presented for the multiple test method only and for both density (including correlated bias errors) and kinematic viscosity.

Density ρ. The precision limit $P_{\bar{\rho}}$, for the result is given by the RSS of the contributions of the precision limits for the individual variables, i.e., equation (25), as

$$P_{\bar{\rho}}^2 = \theta_{D_t}^2 P_{\bar{D}_t}^2 + \theta_{t_t}^2 P_{\bar{t}_t}^2 + \theta_{D_s}^2 P_{\bar{D}_s}^2 + \theta_{t_s}^2 P_{\bar{t}_s}^2 \tag{A.1}$$

with

$$P_{\bar{i}} = \frac{2 \cdot S_{\bar{i}}}{\sqrt{N}} \qquad and \quad S_{\bar{i}} = \left[\sum_{k=1}^{N} \frac{\left(X_i - \overline{X_{\bar{i}}}\right)^2}{N-1} \right]^{1/2} \tag{A.2}$$

The standard deviations $S_{\bar{i}}$, for the individual variables D_t, t_t, D_s, and t_s are provided in Table 2. Substituting for the numerical values in equation (A.1), the precision limit for the density of glycerin is $P_{\bar{\rho}}$ = 17.91 kg/m^3 (1.35% of the measured average density). The estimated precision limit is slightly higher for this case compared to the method using end-to-end data-acquisition and reduction cycles, as shown in Table A.1.

Total uncertainty. Using the estimates for the bias limit provided in Table 4 (including correlated bias errors), the total uncertainty for density is evaluated from equation (24) as

$$U_{\bar{\rho}} = \pm\sqrt{B_{\rho}^2 + P_{\bar{\rho}}^2} = \pm\sqrt{1.22^2 + 17.91^2} = \pm 17.95\ kg/m^3$$

$U_{\bar{\rho}}$ is 1.36% of the measured average density, as shown in Table A.1. Comparison of the estimates in Table A.1 with those shown in Table 4 indicates small differences between the values obtained with the two methods for determining the precision limits; therefore, we can conclude that the end-to-end method should be used for its simplicity and conservation of resources.

Table A.1. Uncertainty estimates for density using multiple test method and individual variable precision limits

Term	End-to-end (data from Table 4, with correlated bias errors)		Individual variables	
	Magnitude	Percentage values	Magnitude	Percentage values
B_ρ	1.22 kg/m^3	0.09% $\overline{\rho}$ 0.47% $U_{\overline{\rho}}^2$	1.22 kg/m^3	0.09% $\overline{\rho}$ 0.46% $U_{\overline{\rho}}^2$
$P_{\overline{\rho}}$	16.91 kg/m^3	1.29% $\overline{\rho}$ 99.53% $U_{\overline{\rho}}^2$	17.91 kg/m^3	1.35% $\overline{\rho}$ 99.54% $U_{\overline{\rho}}^2$
$U_{\overline{\rho}}$	16.95 kg/m^3	1.30% $\overline{\rho}$	17.95kg/m^3	1.36% $\overline{\rho}$

Kinematic viscosity ν_t. The precision limit precision limit $P_{\overline{\nu_t}}$, for the result using the teflon spheres is given by equation (25) as

$$P_{\overline{\nu_t}}^2 = \theta_{D_t}^2 P_{\overline{D_t}}^2 + \theta_\rho^2 P_{\overline{\rho}}^2 + \theta_{t_t}^2 P_{\overline{t_t}}^2 + \theta_\lambda^2 P_{\overline{\lambda}}^2 \qquad \text{(A.3)}$$

where the precision limits for the individual variables are defined by equation (A.2). The standard deviations $S_{\overline{i}}$ for D_t, ρ, and t_t, are provided in Table A.2. The precision limit for λ is zero, because the repeated measurements provided each time the same reading.

Substituting for the measured values in equation (A.3), the precision limit for the kinematic viscosity is $P_{\overline{\nu_t}} = 2.59\times10^{-5}$ m^2/s (3.70% of the measured averaged kinematic viscosity). The estimated precision limit is higher for this case compared to the method using the end-to-end method, as shown in Table 5.a.

Total uncertainty. Using the estimated bias limit provided in Table 5, the total uncertainty for density is evaluated from equation (24)

$$U_{\overline{\nu_t}} = \pm\sqrt{(4.5\cdot10^{-6})^2 + (2.59\cdot10^{-5})^2} = \pm2.63\cdot10^{-5}\, m^2/s$$

$U_{\overline{\nu_t}}$ is 3.72% of the measured average kinematic viscosity, as shown in Table A.2. Similar calculations can be made for the measurements for the steel spheres.

Table A.2. Uncertainty estimates for kinematic viscosity (teflon spheres) using multiple test method and individual variable precision limits

Term	**End-to-end (data from Table 5)**		**Individual variables**	
	Magnitude	Percentage values	Magnitude	Percentage values
$B_{\overline{\nu_t}}$	4.5×10^{-6} m^2/s	0.64% $\overline{\nu_t}$ 16.43% $U^2_{\overline{\nu_t}}$	4.5×10^{-6} m^2/s	0.64% $\overline{\nu_t}$ 3.02% $U^2_{\overline{\nu_t}}$
$P_{\overline{\nu_t}}$	1.01×10^{-5} m^2/s	1.43% $\overline{\nu_t}$ 83.57% $U^2_{\overline{\nu_t}}$	2.59×10^{-5} m^2/s	3.70% $\overline{\nu_t}$ 96.98% $U^2_{\overline{\nu_t}}$
$U_{\overline{\nu_t}}$	1.11×10^{-5} m^2/s	1.57% $\overline{\nu_t}$	2.63×10^{-5} m^2/s	3.72% $\overline{\nu_t}$